Journal of Machine Engineering, Vol. 16 No. 3, 2016

Received: *06 March 2016* / Accepted: *23 May 2016* / Published online: *20 June 2016*

hexapod, characteristic diagram, thermal error, simulated, measured, correction algorithm

Matthias PUTZ[1]
Steffen IHLENFELDT[2]
Bernd KAUSCHINGER[2]
Christian NAUMANN[1*]
Xaver THIEM[2]
Mirko RIEDEL[2]

IMPLEMENTATION AND DEMONSTRATION OF CHARACTERISTIC DIAGRAM AS WELL AS STRUCTURE MODEL BASED CORRECTION OF THERMO-ELASTIC TOOL CENTER POINT DISPLACEMENTS

In milling machines, waste heat from motors, friction effects on guides and most importantly the milling process itself greatly affect positioning accuracy and thus production quality. Therefore, active cooling and lead time are used to reach thermal stability. A cheaper and more energy-efficient approach is to gather sensor data from the machine tool to predict and correct the resulting tool center point displacement. Two such approaches are the characteristic diagram based and the structure model based correction algorithms which are briefly introduced in this paper. Both principles have never been directly compared on the same demonstration machine, under the equal environmental conditions and with the same measurement setup. The paper accomplishes this comparison on a hexapod kinematics examined in a thermal chamber, where the effectiveness of both approaches is measured and the strengths and weaknesses of both are pointed out.

1. INTRODUCTION

Machine tool deformation occurs during operation due to waste heat from motors and frictional heat from guides, joints and the tool, while coolants act to reduce this influx of heat. Additional thermal influences come from the machine tool's environment and foundation. This leads to inhomogeneous, transient temperature fields inside the machine tool which displace the tool center point (TCP) and thus reduce production accuracy and finally the product quality [1]. Active cooling can lessen this effect but does, however, require considerable amounts of energy. Another possibility is to stabilize temperature fields by allowing for lead-time or to limit the waste heat by reducing the operating speed.

[1] Fraunhofer Institute for Machine Tools and Forming Technology IWU, Chemnitz, Germany
[2] Dresden University of Technology TUD, Germany
[*] E-mail: Christian.Naumann@iwu.fraunhofer.de

The Collaborative Research Centers/Transregio 96 (CRC/TR 96), a German Research Foundation (DFG) project, attempts to shift this balance between productivity, energy efficiency and product quality by reducing the impact of waste heat on the TCP positioning accuracy while reducing or even eliminating the need for lead-time and coolants, see [2]. This is done, e.g., by correcting the TCP position through the prediction of its thermo-elastic displacement based on data gathered from various sensors and load data from the machine tool control. One such algorithm is the characteristic diagram based correction which uses high-dimensional characteristic diagrams to directly map discrete points of the temperature field onto the resulting TCP displacement. The structure model based correction uses thermal and thermo-elastic models to obtain correction values through efficient simulation in thermal real time. After examining the relevant thermo-elastic processes and developing the necessary models and algorithms, the CRC/TR 96 now enters its second phase where its focus shifts to the application and test of the achieved results on complex assemblies and demonstration machines under laboratory settings. After a brief introduction of the two correction principles above, the main focus of the paper will therefore be on their application on our hexapod kinematics "MiniHex" shown in Fig. 3 and Fig. 4. The Measurement setup will be detailed, including the multitude of sensors used and how they are applied to guarantee the accuracy of our measurements. Some thermo-elastic properties of the MiniHex will also be explained and the relevant aspects of the implementation of the online correction methods used will be discussed. Characteristic diagram based and structure model based correction will be applied to and tested on the same demonstration machine, the hexapod kinematics "MiniHex". It is ideal for modelling, consisting of six structurally identical translational axes with only slight thermal differences. The precision of this machine is influenced by the thermal expansion of the axes in each axis' feed direction. The effectiveness of both correction approaches is evaluated and compared under specified environmental conditions using the same measurement setup. Thereby the comparability of the different methods is achieved. Finally the coming research in both fields will be outlined.

2. CHARACTERISTIC DIAGRAM BASED CORRECTION

CHARACTERISTIC DIAGRAMS are continuous maps of a set of input variables onto a single output variable. They consist of a grid of support points along with kernel functions which describe the interpolation in between. Equation 1 shows a one-dimensional linear kernel $K_j(T_i)$ between two support points $\hat{T}_j$ and $\hat{T}_{j+1}$ which depends on a temperature T_i

$$K_j(T_i) = \frac{T_i - \hat{T}_j}{\hat{T}_{j+1} - \hat{T}_j} \tag{1}$$

Characteristic diagrams are created by first discretizing each input variable in order to establish the grid, then choosing a type of kernel function adequate for describing the local dependency of the input variables on the output variable and finally calculating the

parameters of the kernel functions for each support point based on training data from simulations or experiments. The most common form of characteristic diagram uses multilinear interpolation between support points, where a scalar factor r_j equal to the output value at the support point acts as a weight multiplied to the pyramid shaped kernel K_j.

$$f(\vec{T}_i) = \sum_j r_j \cdot K_j(\vec{T}_i), \quad \vec{T}_i := (T_{i,1}, \cdots, T_{i,n}) \tag{2}$$

These higher dimensional kernels can be created by simply multiplying one-dimensional kernels. A more detailed account of characteristic diagrams and how they are calculated can be found in [3]. Here Priber describes a method called "Smoothed Grid Regression" (SGR) which adds smoothing terms to the data fitting terms described above in order to fit sparse or defective data. SGR is the basis for the characteristic diagram research presented here.

The most reliable way to predict the tool center point (TCP) displacement is via thermo-elastic finite element (FE) simulation. A CAD model of a given machine tool serves as the basis for this approach. On it an FE mesh is created. After establishing the partial differential equations (PDEs) describing the heat transfer within the machine tool and with its surroundings, FE simulations are run in order to obtain the temperature fields of the machine tool for specified load regimes. Using linear thermo-elastic expansion, the deformation can then be calculated from each temperature field and the displacement of the TCP read from this deformation field, see [4].

Characteristic diagram based TCP correction presents a kind of shortcut to this laborious simulation based approach. Rather than using the entire temperature field and keeping track of its changes, a small selection of points from this field is taken and mapped directly onto the TCP displacement via a characteristic diagram. Each mapping is a single dataset independent of all others so that time is of no concern. Naturally, this only works if the selected points are able to uniquely identify the corresponding temperature field for any given configuration and if enough of these temperature fields are represented in the characteristic diagram to allow reliable interpolation, as shown in [5]. While this shortcut is obviously less precise than a complete simulation, it has several advantages. Characteristic diagrams, once created, are very easy and efficient to apply so that they can be effortlessly incorporated into an online correction. They can also be derived entirely from measurement data so that CAD models and simulations are not necessarily needed. Since they are not time-dependent, the errors made during simulations due to imprecise assumptions have little effect on the characteristic diagrams.

In the course of the CRC/TR 96 project, we have been able to improve characteristic diagram computation by employing multigrid solvers to efficiently solve the large sparse linear systems of high dimensional characteristic diagrams. This was done by developing a PDE that mimicked the common approach (eq. 1 and 2) and using it to derive the linear system via the finite element method (FEM). For piecewise multilinear kernels, this PDE in weak form reads:

$$\forall \overrightarrow{\delta u}: \quad \sum_{i=1}^{nData} (z_i - u(\vec{x}_i)) \cdot \delta u(\vec{x}_i) \quad + \quad \int_\Omega \lambda(\vec{x}) \cdot \nabla u(\vec{x}) \cdot \nabla \delta u(\vec{x}) \, d\vec{x} \quad = \quad 0 \tag{3}$$

The equation comprises of a data fitting term plus a smoothing term. Its derivation along with a more detailed explanation can be found in [2], under chapter "Correction Algorithms and High-Dimensional Characteristic Diagrams". Where the common approach is limited to only 5 or 6 input variables due to limited memory, our new iterative solver can cope with 10 or more variables, as was shown in [6] using simulation data from a machine tool column. This development is of paramount importance when complex machine tool structures are to be modelled.

In many trials we have discovered that multilinear interpolation, given a fine enough grid, is best suited for our thermo-elastic problems. Not only are they sufficiently accurate and easy to calculate, they also require comparatively few parameters and limit the risk of overfitting, see [6]. We will therefore be using it in our experiments described in chapter 4.2.

Another important aspect of characteristic diagram based correction is the optimal selection of input variables. For this purpose, a new algorithm using a least squares estimator was also developed within the CRC/TR 96 and is explained in detail in [7]. It produces a minimal set of input variables that allows the distinction of all relevant temperature states of the machine tool.

3. STRUCTURE MODEL BASED CORRECTION

Structure model based correction presents another way to predict thermal machine expansion to correct TCP displacement. This approach uses models describing the physical behaviour of the machine. The models are based on the geometry of the machine and also describe structural variations due to relative movements between assemblies. One advantage of this approach is that these models are valid for a broad variety of load cases and ambient conditions. The necessary functions for the structure model based correction can be divided into modules [8]. Figure 1 shows the chain of modules. Another way to implement a structure model based correction can be found in [9].

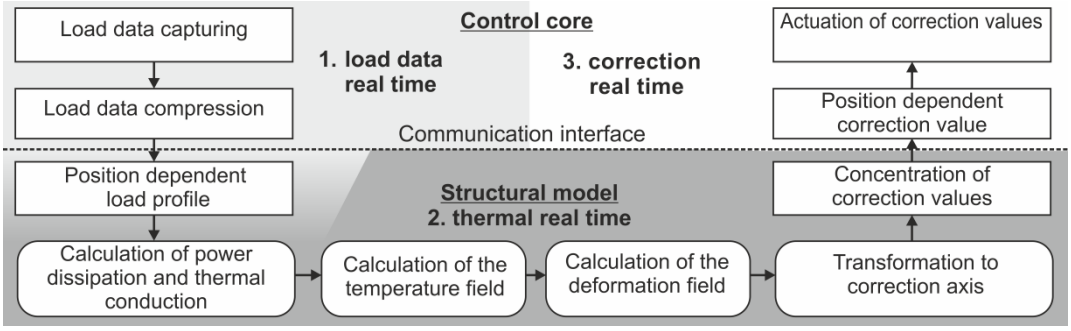

Fig. 1. Modules of structure model based correction of thermal errors

FE models and node models were used. These models need to describe the thermal state of the machine tool sufficiently well at all times. They must therefore be calculated in

thermal real time which is characterized by the smallest thermal time constant of the machine tool (in the most cases some minutes). If an FE model is used, typically the model order has to be reduced [10] or the FE mesh coarsened [11] to fulfil this requirement.

To calculate the temperature field of the machine tool, the thermal model requires heat flows (power dissipation), thermal conduction and the ambient temperature as load data. The time dependent power dissipation and thermal conduction are calculated based on data from the machine control (axis positions, velocities, motor torques), see [2] pp. 185-198. The largest uncertainties are in the parameters power dissipation and thermal conduction [12]. In addition to the control data, only one temperature sensor is necessary to measure the ambient temperature. Structure model based correction is particularly advantageous if no temperature sensors can be placed near the relevant positions on the machine and they save the costs for additional sensors. This also makes it resistant to broken or faulty sensors and thus easier to install and maintain.

Control data is captured in high resolution (typically milliseconds) to detect load peaks. High resolution is also required to assign the power dissipation in moving assemblies to the right elements in the thermal model ("position dependent load profile" in Fig. 1. For example, the power dissipation because of friction at a profile rail has to be assigned to the current position of the guide carriage. Therefore, the thermal model and the load data acquisition have two different real time domains. The first real time domain with high real time requirements is for load data acquisition and the second domain is thermal real time (model calculation), which has low real time requirements (cycle times up to minutes) [13].

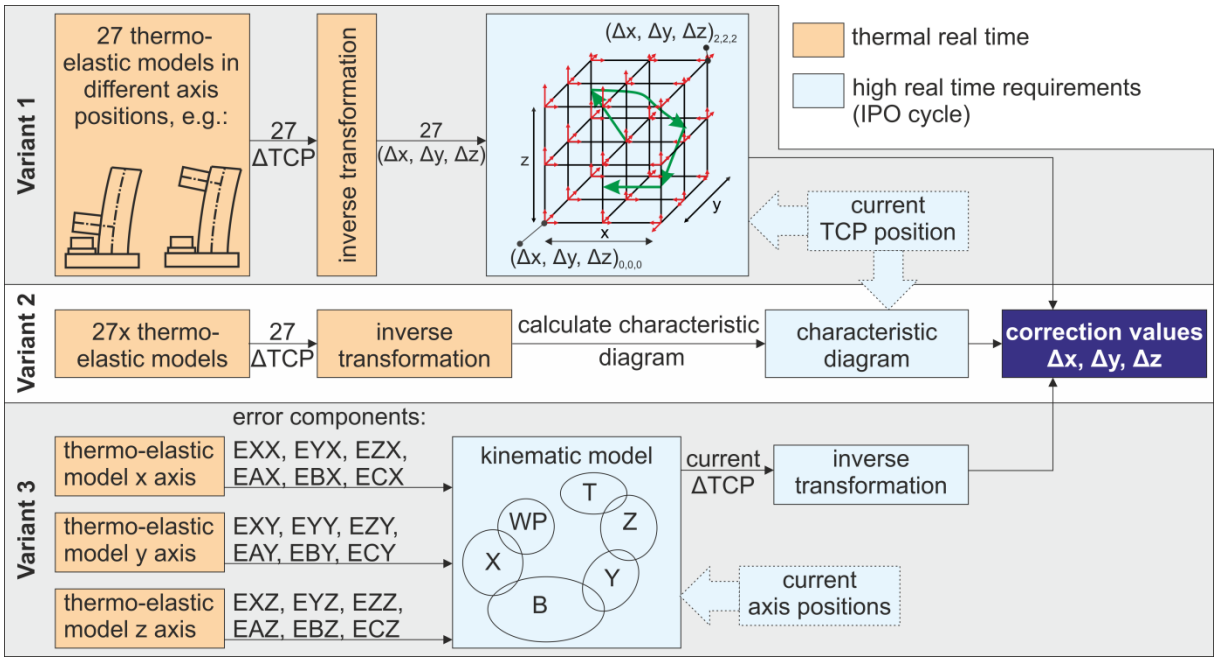

Fig. 2. Variants for calculating position-dependent correction values under high real rime requirements

In the thermo-elastic model (e.g. FE model), the temperature field is used to calculate the deformation field of the machine tool. Typically, model order reduction is not necessary for thermo-elastic models because they are already able to calculate the deformation in

thermal real time. The displacement at the TCP can be read from the deformation field. This displacement depends on the axis positions. These positions can change within an interpolation cycle (IPO cycle) of the control. That is why the correction values also have to be calculated and actuated in one IPO cycle (third real time domain [13]). In contrast to characteristic diagram based correction it is not possible to process all necessary functions within an IPO cycle. The computing time to rebuild and calculate the thermo-elastic model with the position changes is typically too large for one interpolation cycle. Three different ways of solving this problem are sketched in Fig. 2 on the example of a three axis machine.

The first variant is to use a grid of support points within the workspace of the machine. The correction values for the axes have to be determined by interpolation between support points depending on the current TCP-Position ([2] pp. 185–198).

The second variant is to use characteristic diagrams to map the correction values for the axes onto the TCP. This must not be confused with characteristic diagram based correction. Characteristic diagram based correction uses characteristic diagrams to map the TCP displacement onto measured temperatures. In both cases characteristic diagrams are used to fulfil high real time requirements.

A third variant is to calculate the error components [14] of all axes for a number of support points along each axis instead of calculating the deformation field of the whole machine at once. With the help of a kinematic model it is then possible to determine the thermal error at the TCP. The kinematic model is represented by a kinematic chain of workpiece (WP), x axis (X), base (B), y axis (Y), z axis (Z) and the tool (T). Li used this variant for the compensation of geometric and thermal errors on a vertical machining center [15]. To calculate the current displacement at the TCP (ΔTCP), the current axis positions are needed. Then the correction values for the individual axes are calculated from the TCP displacement via an inverse transformation.

The final step in any correction approach is to actuate the correction values by adding them as offsets to the commanded axis coordinates.

4. IMPLEMENTATION AND TEST

4.1. DEMONSTRATION MACHINE “MINIHEX” AND THE EXPERIMENTAL SETUP

A validation of our correction methods was done on the portable demonstration machine "MiniHex", a stewart-platform that can position its movable platform in six degrees of freedom in a 600 x 600 x 400 mm workspace (see Fig. 3).

The structure of this machine is fixed on a massive support frame. Each of the six translational axes is driven by an induction motor, connected by a toothed drive belt to a spindle. The spindles are rotated using a ball bearing. Their rotation drives the ball nut and the adjoined distance tube. Each of these translational axes is connected by universal joints to the support frame and the movable platform. The thermally relevant components of the MiniHex are the drives, the spindle bearings, the ball nuts, the spindles and the distances tubes.

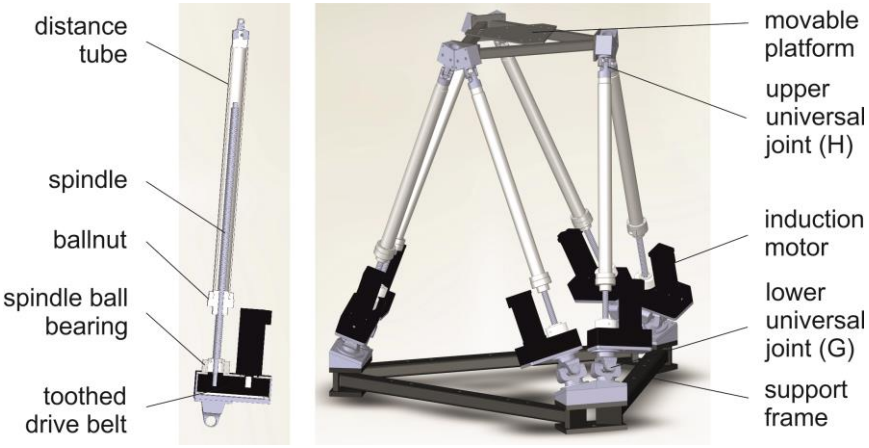

Fig. 3. Structure and components of the MiniHex

Due to their structure and make-up, the joints on either end of each axis can be regarded as thermal insulation between the support frame, the axes and the platform. The thermal expansion of the structure occurs mainly in the spindle and the distance tube. Because the position of each axis is only measured indirectly by "counting" the rotations of the spindle, the thermo-elastic expansion of the axis cannot be directly detected and compensated. The parallel kinematic structure of the MiniHex turns the expansion of the six axes into a complex displacement of the platform in all six degrees of freedom. To reliably measure the thermo-elastic expansion of the axes and thus the displacement of the platform, the experiments on the MiniHex were conducted inside a thermal chamber with a constant 20°C and constant humidity and illumination. Due to the thermally insulating joints, this ensured that the support frame and the platform also remained at a constant 20°C and could therefore be disregarded. The experimental setup we used is shown in Fig. 4.

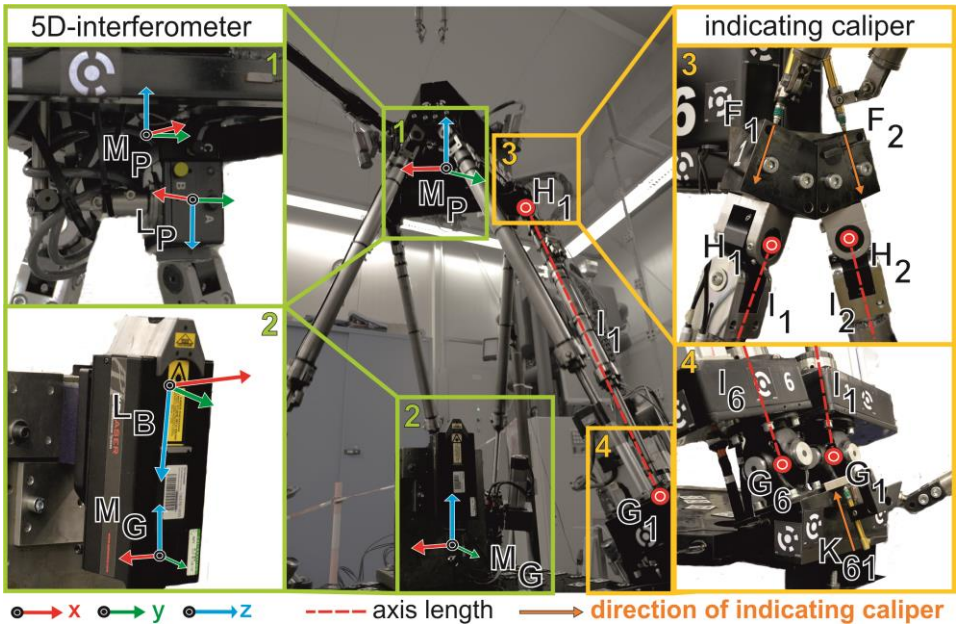

Fig. 4. Experimental setup for thermal axis expansion detection on the MiniHex

The main measurement of the platform position was done using the 5D laser interferometer XD6 from API. As a control measurement, we installed indicating calipers (F_1, F_2,..., F_6) with a range of 1 mm near the upper universal joins (H_1, H_1 ... H_6) so that they could measure the expansion in the top most position (0, 0, 260) directly above the laser interferometer. To make sure that the support frame remained unchanged, three additional indicating calipers (K_{61}, K_{23}, K_{45}) were installed at the bottom end of the axes.

Since the indicating calipers could not be placed directly at the axis joint centers and the expansion of the axes effects a complex displacement of the platform, a transformation matrix M had to be found to convert the distances f measured by the indicating calipers into the desired axis expansion *l*:

$$\vec{l} = M \cdot \vec{f} \tag{4}$$

To compute matrix *M*, we extended each axis alone and in combination with others near the position (0, 0, 260) by small positive and negative increments. From about 40 different positions that were measured with both the calipers and the laser interferometer, matrix *M* was determined as:

$$M = \begin{bmatrix} 0.874 & 0.079 & 0.020 & 0.025 & -0.022 & 0.034 \\ 0.100 & 0.881 & 0.024 & -0.019 & -0.001 & 0.039 \\ -0.051 & 0.073 & 0.870 & 0.103 & 0.022 & 0.013 \\ -0.022 & 0.046 & 0.089 & 0.922 & 0.026 & -0.026 \\ 0.021 & 0.004 & -0.023 & 0.039 & 0.874 & 0.110 \\ 0.024 & -0.014 & 0.004 & 0.030 & 0.096 & 0.885 \end{bmatrix} \tag{5}$$

The fact that the main diagonal elements are all around 0.9 whereas all off-diagonal elements are small proves the good transfer behavior of indicating caliper and laser interferometer. Off-diagonal elements of up to 0.11 show that crosstalk indeed occurred.

The 5D laser interferometer is able to determine the location of its counterpart mounted on the platform in five degrees of freedom, namely the x, y and z position and the rotation around the x (A) and y axis (B). The rotation around the z axis (C) cannot be measured so that the platform position must be maintained close to C=0. The conversion of the coordinates *i* measured by the laser interferometer to axis expansion *l* can similarly be done using another transformation matrix M:

$$\vec{l} = M \cdot \vec{i} \tag{6}$$

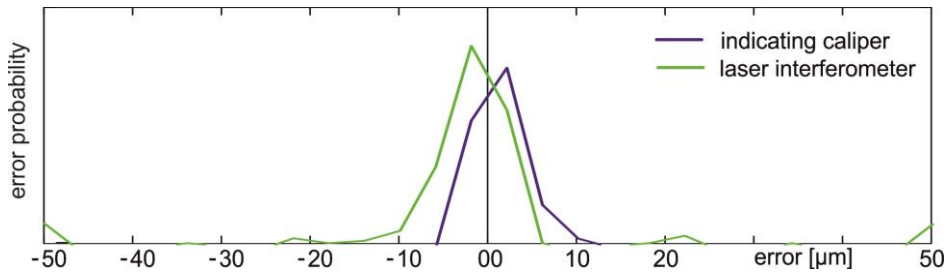

Fig. 5. Histogram of the deviations between measured and commanded axis lengths

Figure 5 shows the frequency distribution of axis length deviations for both the laser interferometer and the indicating calipers compared to the commanded position (0, 0, 260) of the machine control. The expected value of both is about 3µm away from the commanded position which itself has a positioning accuracy of 3µm. Small differences in axis lengths lead to a similar frequency distribution with a variation of about 5 µm. Larger differences, however, prevent the accurate reconstruction of the axis lengths because of the unknown C-angles and show errors ranging from 20 µm to 50 µm.

4.2. VALIDATION OF CHARACTERISTIC DIAGRAM BASED CORRECTION

Validating the characteristic diagram based correction requires gathering enough training data to describe all relevant temperature states of the demonstration machine, using that data to calculate a characteristic diagram and then testing its quality of approximation by gathering test data and comparing the displacement measured in the test data to that which the characteristic diagram prognoses.

Both training and test data comprise of the following variables (compare Fig. 3):

- Tb_i … temperature bearing of axis *i*,
- Tn_i … temperature nut of axis *i*,
- Tt_i … temperature tube of axis *i*,
- Tp_i … temperature platform near end of axis *i*,
- Te … temperature of environment, omitted since it is constant by design,
- Lc_i … commanded length of axis *i*,
- dL_i … = $Lr_i - Lc_i$ … length change with Lr_i measured (real) length of axis *i*.

Since the thermo-elastic expansion of each axis of the parallel kinematic MiniHex is quasi-independent of the temperature fields of all five other axes, we are able to compute the expansion of each axis *i* in a separate characteristic diagram which maps:

$$\forall i = 1..6: \quad (Tb_i, Tn_i, Tt_i, Tp_i, Te, Lc_i) \quad \rightarrow \quad dL_i \tag{7}$$

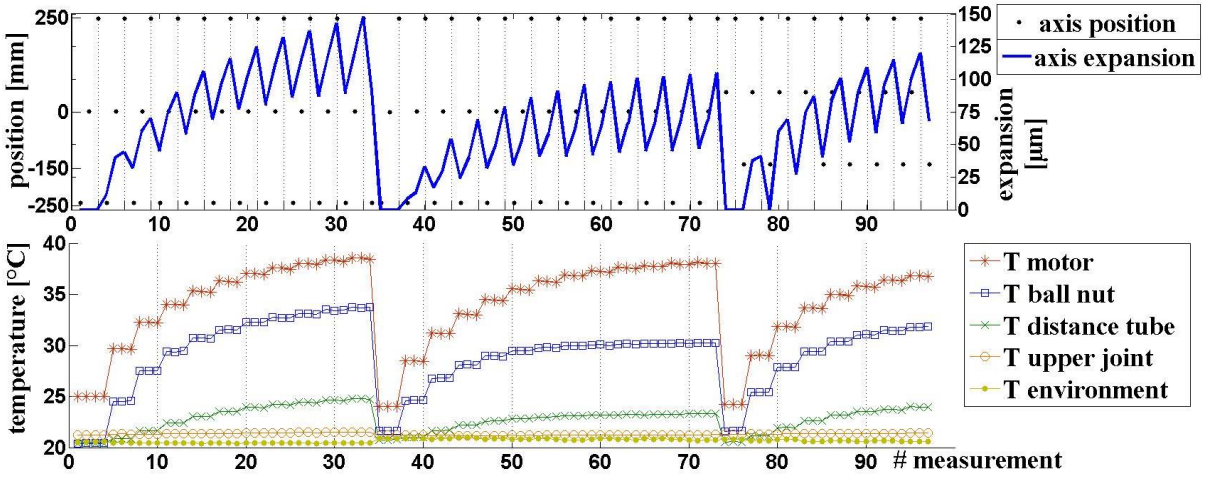

Fig. 6. Measurement data from MiniHex experiments

In our experiments, we moved the platform of the MiniHex up and down periodically at about 30 m/min. This induced frictional heat into spindles and distance tubes and the waste heat from the motors flowed likewise into the spindles. Figure 6 shows the temperatures, axis positions and elongation of axis 1 for two experiments (measurements N° 1-34 heating in interval 10…240 mm and N° 35-73 heating in -10…-240 mm) designed for characteristic diagram training and one for its evaluation (measurements 74-97).

Figure 6 shows that the temperature of both platform and environment did not change notably during the experiment, as expected. Therefore they hold no value for characteristic diagram based correction and can be omitted. The resulting piecewise linear characteristic diagram with 4 input dimensions allowed the predictions of the thermic elongation of axis 1 shown in Fig. 7.

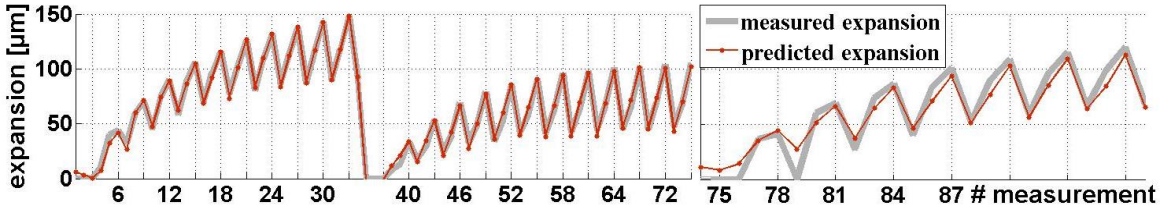

Fig. 7. Training (left) and test data fitting (right) of thermic MiniHex axis elongation

Figure 7 compares the measured axis elongation (gray) to the one predicted by the characteristic diagram (black) for the training data (left) from which the characteristic diagram was created and the test data (right). The training data was reproduced almost exactly as measured, whereas the training data displays some deviation particularly in the middle position (+55 mm) and at the beginning of the measurement. These errors exist for two main reasons. Sensor placement was predetermined and chosen specifically for simulation parametrization. They are not ideal for characteristic diagram based correction since they do not produce a detailed view of the temperature distribution along the spindle and distance tube. The other problems arise from the restrictions of the displacement measurement via laser interferometer. We were only able to automatically measure at equidistant intervals along the direct line of the laser where all measurement points had to also be outside the interval we used for heat generation. Due to these restrictions measurements were lengthy and many would be needed for a complete representation of all relevant thermal states of the MiniHex. Even so, we were able to reduce the thermal error from 120 µm to below 25 µm. More experiments for training data acquisition would bring some additional improvement but a flawless prediction could only be achieved by installing additional temperature sensors.

4.3. VALIDATION OF STRUCTURE MODEL BASED CORRECTION

The aim of the conducted experiments was to compare the simulated thermal errors from structure model based correction to measurements and the results from characteristic diagram based correction. The precision of the thermal model of the MiniHex was shown in

[2] pp. 69-84. There the simulation was run in thermal real time based on control data and the simulated temperatures matched the measured values very well. Until now the simulated thermal errors had not been compared directly to measurements. To improve the accuracy of the MiniHex, only the error components in axis directions are relevant (Fig. 2, Variant 3).

As load cycle for the experiment all axes move identically due to the restrictions of the laser interferometer. That is why all axes have nearly the same thermal load, except for dissimilar pretensioning. The axes were moved periodically over a period of 110 min to heat them up. The control data of the six axes were captured with a sampling time of 10 ms. The ambient temperature is recorded every 1s. With this input data, the power dissipation, thermal conduction and the thermal model are calculated. The resulting simulated temperatures in axis 1 are compared to three PT100 resistance temperature sensors. The first temperature sensor is on the bearing of the spindle of the ball screw. The second temperature sensor is on the spindle nut and the last one is on top of the middle of the distance tube. The results are shown in Fig. 8. Some simulated temperatures deviate strongly from the measurements, most notably at the spindle nut. The main reason for this discrepancy is that the parameters of the power dissipation and thermal conduction models were adjusted for another machine state. The experiments for parameter adjustment had been carried out with a higher preload of the spindle nut and less fill quantity of grease. The nut's preload was changed during maintenance. This preload, especially, has a great effect on the torque friction in the spindle nut. That's why the simulated temperature is up to 6 K higher than the measured temperature at the nut. In conclusion, for the use of structure model based correction of thermal errors it is necessary to adjust the model parameters so that they describe the current state of the machine. The simulated temperature at the distance tube meets the measured temperature quite well, except in the time range of 110 to 130 minutes. The machine halts after 110 minutes and the heat transfer to the environment slows down. Forced convection at the distance tube stops and only free convection remains. The high nut temperature and the decreased conduction lead to an initial short increase in tube temperature in the simulation model right after the machine stops. The effect can also be seen in the measurements, however less strongly. The reasons for the different amplitudes are the lower real temperature of the nut and perhaps a slight air current in the thermal chamber which increased the convection.

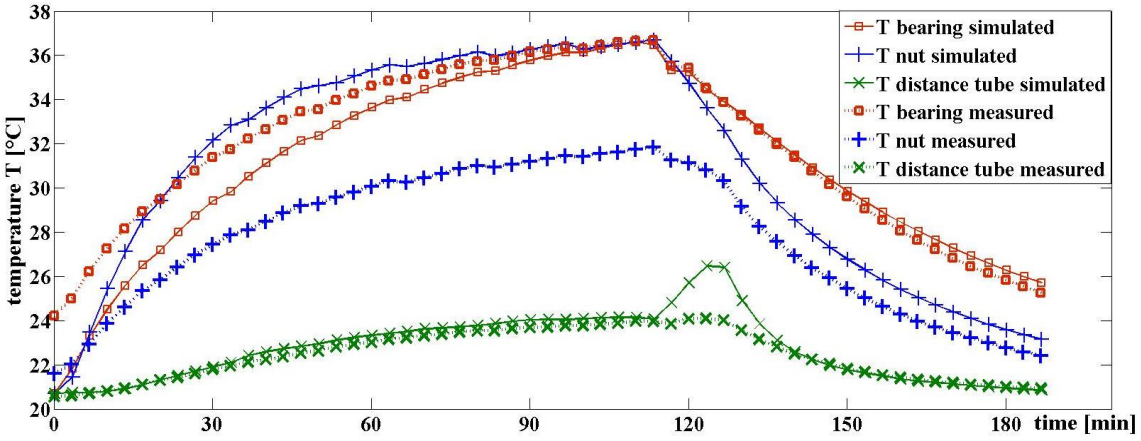

Fig. 8. Temperatures of axis 1 of the MiniHex

Another reason for the temperature differences of nut and bearing between simulation and measurement is that the simulation model starts at a homogenous 20°C. The MiniHex was already slightly warm near the bearings at the beginning of the measurement because of previous movements performed in setting up the measurement. After approximately 30 minutes the simulated bearing temperature reaches the measured temperature. The simulation model approaches the real temperature even if the start temperatures deviate from the real temperature. This is one advantage of the structure model based correction.

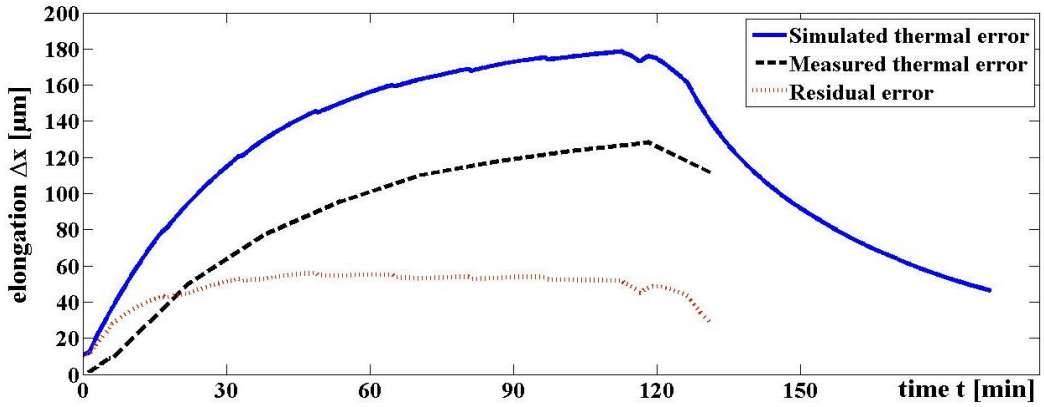

Fig. 9. Simulated and measured thermal error for axis 1 in fully extended position

In Fig. 9, the thermal error for the fully extended axis 1 (+260 mm) of the MiniHex is shown. The other five axes are similar. Since the simulated temperature is higher than the measured temperature, the simulated thermal error is also greater. This diagram shows that the preload of the spindle nut has a great effect on the thermal error. At the start of the experiment, the residual error rises until it stabilizes around 50 µm after 30 minutes. In this example, the thermal error can be reduced by up to 60% through the structure model based correction. Even using a simulation model with unadjusted parameters, this still improved the accuracy of the MiniHex. By adjusting the parameters of the power dissipation in the spindle nut, significant improvements in the simulation results are possible. A comparison of the adjusted structure model based correction to characteristic diagram based correction for the test measurement above can be seen in Fig. 10.

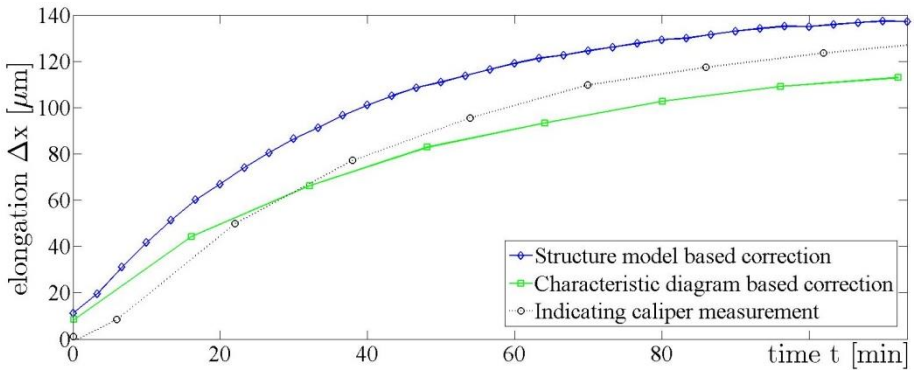

Fig. 10. Comparison of correction methods for test experiment (see Fig. 6, N° 74-97)

5. CONCLUSION

The main purpose of this paper was to assess the current state of characteristic diagram based and structure model based correction through precision experiments in a controlled environment. The device under test was the stewart-platform "MiniHex". Through a combination of indicating calipers and a 5D laser interferometer, a very exact measurement of the current axis position was achieved for all configurations with approximately equal axis lengths. Future experiments will explore the possibility of measuring platform movement through a set of cameras in combination with reference markers in order to be more flexible in experimental design.

Two experiments for gathering training data provided the basis for a characteristic diagram which was then tested in a third, independent experiment. The characteristic diagram delivered good predictions for the thermo-elastic axis expansion and was able to reduce the thermal error from 120 µm to below 25 µm. Follow-up experiments will determine the impact of varying ambient temperatures on prediction quality.

With structure model based we were already able to correct up to 60% of the thermal errors of the spindle axis without any parameter adjustment of the models. However, there is still a high potential for improvement through parameter adjustment with additional experiments. Only one or two different load cases are needed to determine the power dissipation caused by friction between the spindle nut and the ball screw spindle. As shown in the experiments, power dissipation through friction has a great influence on the simulated thermal errors. The amount of measurements needed for this approach is still less than that for correlative correction approaches. In further investigations, structure model based correction with adjusted model parameters will be compared to measured displacements.

ACKNOWLEDGMENTS

This research was supported by a German Research Foundation (DFG) grant within the Collaborative Research Centers/Transregio 96, which is gratefully acknowledged. Additional thanks go to Carsten Richter and Andy Creutziger from the Fraunhofer IWU and Steffen Schröder from the Dresden University of Technology who supported us with our experiments on the MiniHex.

REFERENCES

[1] BRYAN J., 1990, *International status of thermal error research*, CIRP Annals - Manufacturing Technology, 39/2, 645-656.
[2] GROSSMANN K. et al., 2015, *Thermo-energetic design of machine tools*, Springer.
[3] PRIBER U., 2003, *Smoothed grid regression*, proceedings workshop fuzzy systems, 13, Dortmund.
[4] MAYR J. et al., 2009, *Compensation of thermal effects on machine tools using a fdem simulation approach*, 9th International Conference and Exhibition on LASER Metrology, Machine Tool, CMM and Robotic Performance, London.
[5] NAUMANN C., PRIBER U., 2012, *Modellierung des Thermo-Elastischen Verhaltens von Werkzeugmaschinen mittels Hochdimensionaler Kennfelder*, Proceedings Workshop Computational Intelligence, Dortmund.
[6] NAUMANN C. et al., 2015, *Characteristic diagram based correction algorithms for the thermo-elastic deformation of machine tools*, Proceedings 48th CIRP Conference on Manufacturing Systems, Naples.

[7] HERZOG R., RIEDEL I., 2015, *Sequentially optimal sensor placement in thermo-elastic models for real time applications*, Optimization and Engineering, 16/4, 737-766.
[8] GROSSMANN K., MÜHL A., THIEM X., 2014, *Modular control integrated correction of thermoelastic errors of machine tools based on the thermoelastic functional chain*, Advanced Materials Research, 1018, 411-418.
[9] ESS M., 2012, *Simulation an compensation of thermal errors of machine tools*, Dissertation, ETH Zurich.
[10] GALANT A., GROSSMANN K., MÜHL A., 2011, *Model order reduction for thermo-elastic models of frame structural components on machine tools,* in ANSYS Conference & 29th CADFEM Users' Meeting Stuttgart.
[11] GALANT A. et al., 2012, *Berechnung von Temperaturfeldern an Werkzeugmaschinen. Vergleichende Untersuchung alternativer Methoden zur Erzeugung kompakter Modelle*, ZWF Zeitschrift für wirtschaftlichen Fabrikbetrieb, 107/6, 457-461.
[12] KAUSCHINGER B., SCHRÖDER S., 2015, *Uncertain parameters in thermal machine-tool models and methods to design their metrological adjustment process*, Applied Mechanics and Materials, 794, 379-386.
[13] GROSSMANN K. et al., 2015, *Challenges in the development of a generalized approach for the structure model based correction,* Applied Mechanics and Materials, 794, 387-394.
[14] ISO 230-1 : 1996, *Prüfregeln für Werkzeugmaschinen Teil 1: Geometrische Genauigkeit von Maschinen, die ohne Last oder unter Schlichtbedingungen arbeiten*, Beuth, July, 1999.
[15] FAN K. et al., 2015, *Integrated geometric and thermal error modeling and compensation for vertical machining centers,* The International Journal of Advanced Manufacturing Technology, 76/5-8, 1139-1150.